Journal of Biomolecular NMR, **22:** 9–20, 2002.
KLUWER/ESCOM

MQ-HCN-based pulse sequences for the measurement of $^{13}C1'$-$^{1}H1'$, $^{13}C1'$-^{15}N, $^{1}H1'$-^{15}N, $^{13}C1'$-$^{13}C2'$, $^{1}H1'$-$^{13}C2'$, $^{13}C6/8$-$^{1}H6/8$, $^{13}C6/8$-^{15}N, $^{1}H6/8$-^{15}N, $^{13}C6$-$^{13}C5$, $^{1}H6$-$^{13}C5$ dipolar couplings in ^{13}C, ^{15}N-labeled DNA (and RNA)

Jiangli Yan, Takeshi Corpora, Padmanava Pradhan & John H. Bushweller*
Department of Molecular Physiology and Biological Physics, University of Virginia, Charlottesville, VA 22908-0736, U.S.A.

Received 18 May 2001; Accepted 15 October 2001

Key words: DNA, nuclear magnetic resonance (NMR), RNA

Abstract

A suite of multiple quantum (MQ) HCN-based pulse sequences has been developed for the purpose of collecting dipolar coupling data in labeled nucleic acids. All the pulse sequences are based on the robust MQ-HCN experiment which has been utilized for assignment purposes in labeled nucleic acids for a number of years and provides much-needed resolution for the dipolar coupling measurements. We have attempted to collect multiple couplings centered on the $^{13}C1'$ and $^{13}C6/8$ positions. Six pulse sequences are described, one each for measurement of one-bond $^{13}C1'$-$^{1}H1'$ and $^{13}C6/8$-$^{1}H6/8$ couplings, one for measurement of one-bond $^{13}C1'$-^{15}N and two-bond $^{1}H1'$-^{15}N couplings, one for measurement of one-bond$^{13}C6/8$-^{15}N and two-bond $^{1}H6/8$-^{15}N couplings, one for measurement of one-bond $^{13}C1'$-$^{13}C2'$ and two-bond $^{1}H1'$-$^{13}C2'$ couplings, and one for measurement of one-bond $^{13}C6$-$^{13}C5$ and two-bond $^{1}H6$-$^{13}C5$ couplings in the bases of C and T. These sequences are demonstrated for a labeled 18 bp DNA duplex in a 47 kDa ternary complex of DNA, CBFβ, and the CBFα Runt domain, thus clearly demonstrating the robustness of the pulse sequences even for a very large complex.

Introduction

Recently, the development of methods to introduce modest degrees of alignment of macromolecules in solution has permitted the measurement of residual dipolar couplings (Tjandra and Bax, 1997). Residual dipolar couplings are a rich source of structural information. The study of DNA structure in solution has always been hampered by the paucity of NOE data that can be obtained for the structure determination, resulting in inadequate constraints to uniquely define the DNA conformation. Recently, Tjandra et al. (2000) have demonstrated that the use of residual dipolar coupling information can dramatically improve the quality of the structures of DNA oligomers. The spectral resolution, particularly in labeled DNA as well as RNA, tends to be quite poor, making it difficult to collect the necessary dipolar coupling data. Tjandra et al. (2000) overcame this in their study of a DNA dodecamer by way of extensive chemical synthesis of DNA molecules with different labeling patterns. While this approach is clearly feasible, it is labor-intensive and expensive. We have sought methodology to permit us to collect multiple couplings from a single sample and thereby obviate the need for multiple samples.

One of the early steps in the assignment process of any labeled oligonucleotide involves correlating the C1′-H1′ of the ribose ring to the C6-H6 and C8-H8 moieties of the aromatic rings within the nucleotide. This is an essential step in the sequential assignment process and forms the basis for further assignments. Such correlations are obtained on the basis of so-called HCN experiments which correlate C1′-H1′ and C6-H6 or C8-H8 moieties to their attached nitrogens (N1

*To whom correspondence should be addressed. E-mail: jhb4v@virginia.edu

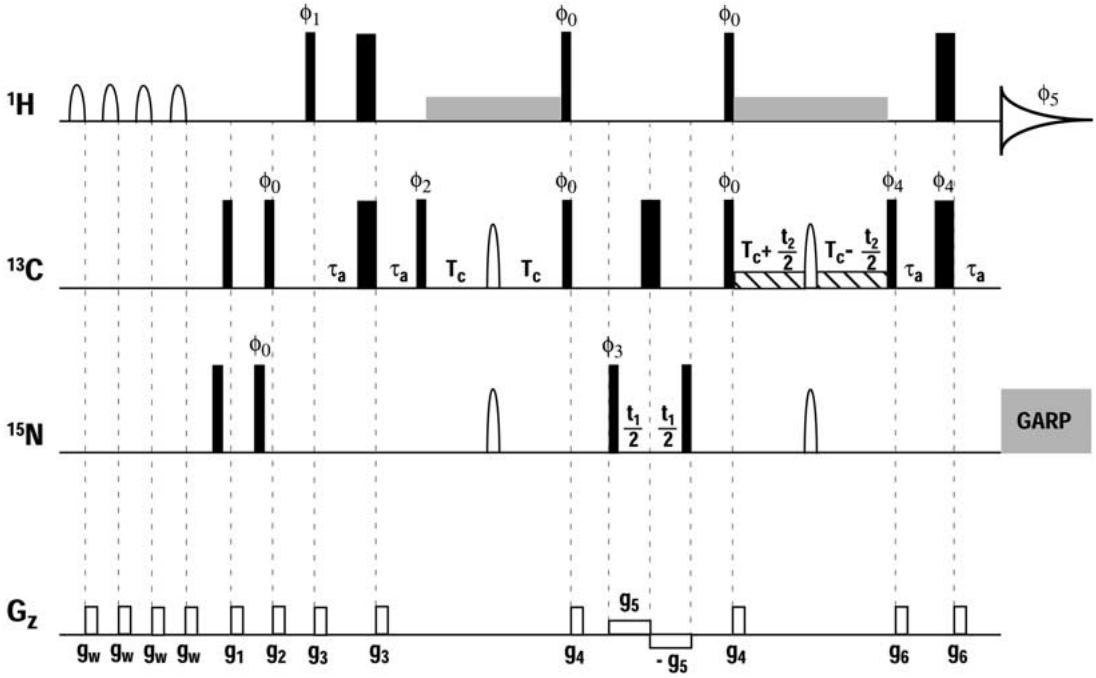

Figure 1. Pulse sequences of the MQ-HCN experiments utilized for measurement of the C1′-H1′ and C6/8-H6/8 dipolar couplings. C1′-H1′ experiment: Narrow and wide black bars represent nonselective 90 and 180 degree pulses, respectively. Prior to the start of the sequence, a WET4 solvent suppression scheme (Smallcombe et al., 1995) was applied. All proton pulses were applied with a field strength of 25 kHz with the exception of the shaped pulses utilized in the WET sequence. Carbon 90 degree pulses were applied with a field strength of 18 kHz with the carrier centered at 86.6 ppm. The selective ^{13}C 180 deg pulses during the constant-time periods were applied as 2.0 ms REBURP pulses at 600 MHz. Nitrogen 90 degree pulses were applied with a field strength of 9 kHz with the carrier centered at 150 ppm. The shaped nitrogen 180 deg pulses during the constant time periods were applied as 1.0 ms hyperbolic secant pulses with a bandwidth of 50 ppm to achieve selective inversion of pyrimidine N1 and purine N9 resonances. Selective WURST2 decoupling on carbon centered at 40 ppm with a bandwidth of 14.5 ppm was utilized during the constant time periods (indicated as hashed boxes) to decouple C2′ nuclei during the second constant time period. The ^{1}H spinlocks were applied at 9 kHz with the ^{1}H carrier moved 0.6 ppm downfield from the water resonance for the duration of each spinlock period. GARP decoupling on nitrogen was used during the detection period. The delays were set as follows: $\tau_a = 1.4$ ms, $T_c = 15$ ms. The phase cycling employed was as follows: $\phi_0 = \{y\}$, $\phi_1 = \{x, x, x, x, -x, -x, -x, -x\}$, $\phi_2 = \{x, -x\}$, $\phi_3 = \{x, x, -x, -x\}$, $\phi_4 = \{x\}$, $\phi_5 = \{x, -x, -x, x, -x, x, x, -x\}$. In addition, ϕ_3 and ϕ_4 are incremented in a States-TPPI manner to obtain quadrature detection in the ^{15}N and ^{13}C dimensions, respectively. Gradient strengths and durations were as follows: $g_w = 16$ G/cm, 2 ms; $g_1 = 6$ G/cm, 0.5 ms; $g_2 = 4.3$ G/cm, 0.5 ms; $g_3 = 4.0$ G/cm, 0.5 ms; $g_4 = 4.0$ G/cm, 1.0 ms; $g_5 = 1$ G/cm; $g_6 = 4.0$ G/cm, 0.5 ms. C6/8-H6/8 experiment: All parameters for the C6/8-H6/8 experiment were identical to the C1′-H1′ experiment with the exception of the position of the ^{13}C carrier, the position of the ^{1}H carrier during the spinlock periods and the length of the ^{13}C REBURP pulse during the constant-time periods. The ^{13}C carrier was positioned at 139.9 ppm. For the ^{1}H spinlock periods the ^{1}H carrier was moved 2.7 ppm downfield of the water resonance. The ^{13}C REBURP pulses were of a duration of 2.1 ms at 600 MHz.

or N9). As the C1′ chemical shift dispersion is often relatively poor and the carbon dispersion for each of the base moieties can be unfavorable as well, this has proven to be a powerful strategy for obtaining these assignments via the relatively favorable nitrogen chemical shift dispersion. HCN pulse sequences have been reported by a number of groups previously (Farmer et al., 1993, 1994; Sklenar et al., 1993a, b, 1998; Tate et al., 1994; Marino et al., 1997; Fiala et al., 1998) and TROSY versions of the HCN experiment have also been described (Fiala et al., 2000).

We have made modifications to the MQ-HCN experiment to permit the measurement of a significant number of dipolar couplings centered on both the C1′ and C6/8 nuclei. Six experiments are described which permit the recording of a total of 10 different types of dipolar couplings in the labeled DNA. The dispersion of the MQ-HCN experiment makes possible the recording of this data on a single sample. The experiments are demonstrated for a ^{13}C/^{15}N-labeled 18 bp DNA duplex in a 47 kDa ternary complex with the CBFβ and the CBFα Runt domain. We show that, even for this large complex, the described experiments

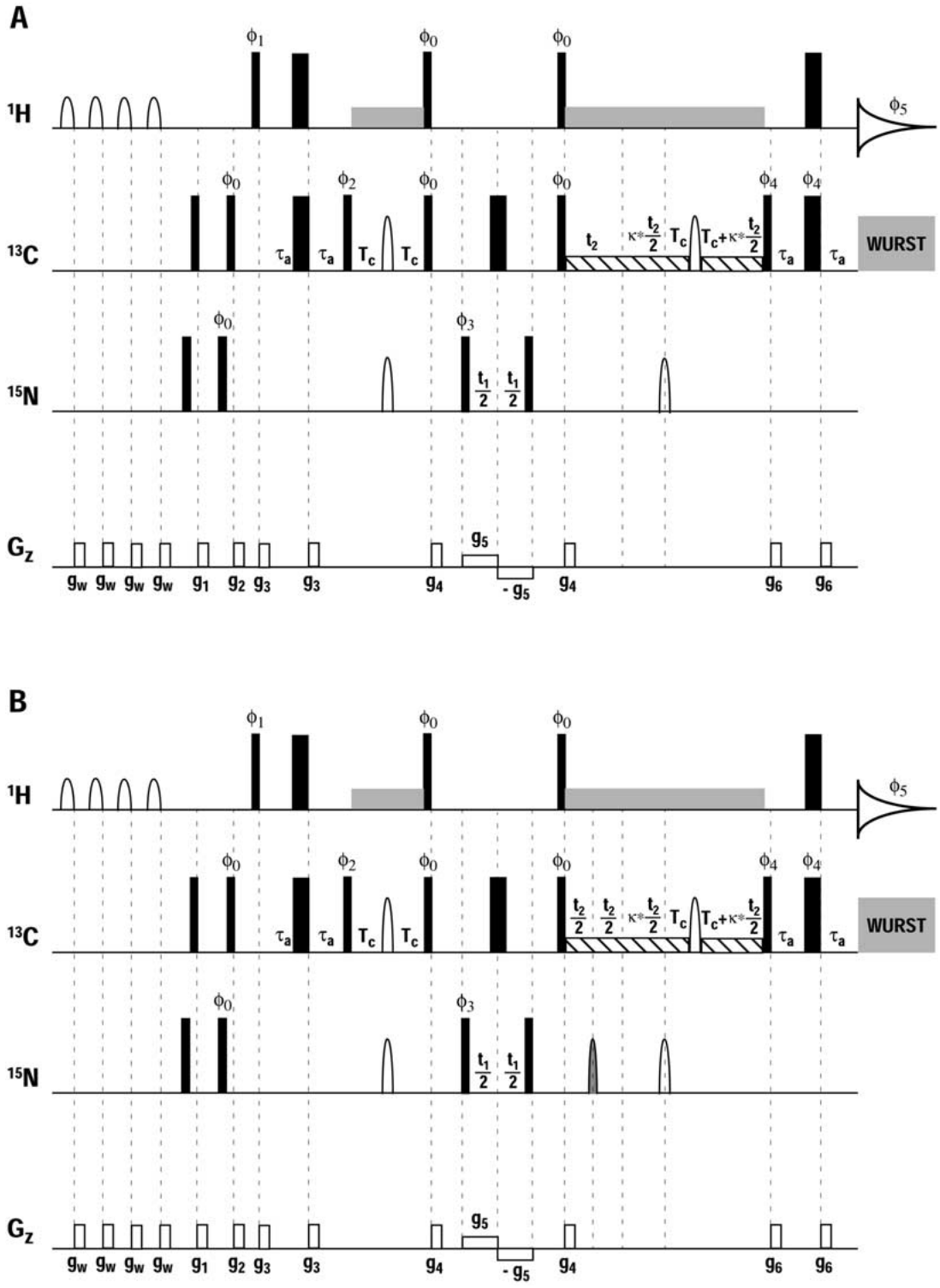

Figure 2. Pulse sequences utilized for the measurement of the one bond C1′-N (A) and C6/8-N (B) couplings as well as two-bond H1′-N and H6/8-N couplings. (A) C1′-N (H1′-N) experiment. The parameters are identical to those listed above for the C1′-H1′ experiment with the exception of the changes described below. A parameter κ has been added for scaling of the one-bond C1′-N coupling. A value of $\kappa = 4$ has been utilized in all experiments. WURST decoupling on ^{13}C was applied during acquisition. (B) C6/8-N (H6/8-N) experiment. The parameters are the same as those listed above for the C6/8-H6/8 experiment with the exception of the changes described below. A parameter κ has been added for scaling of the one-bond C1′-N coupling. A value of $\kappa = 4$ has been utilized in all experiments. A selective 180 degree pulse is applied to the N7 nuclei of A and G during the initial t_2 period. The selective N pulse was applied as a 1.5 ms ISNOB3 pulse modulated to effect a 180 deg pulse 75 ppm downfield of the ^{15}N carrier position, corresponding to the chemical shift of the N7 nuclei of A and G. WURST decoupling on ^{13}C has been applied during acquisition.

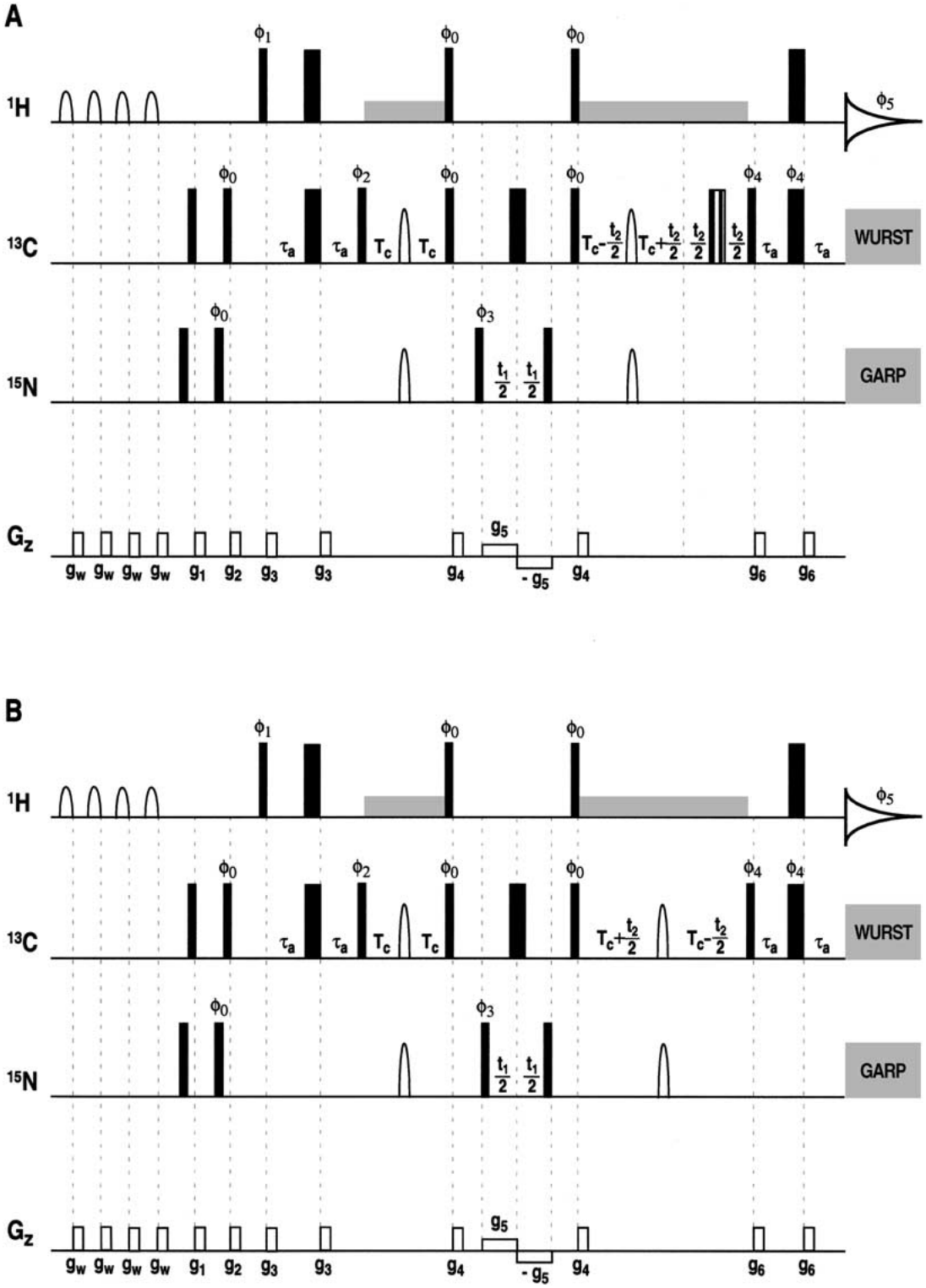

Figure 3. Pulse sequences used for measurement of the one-bond C1′-C2′ (A) and C6-C5 (B) as well as two-bond H1′-C2′ and H6-C5 couplings. (A) C1′-C2′ (H1′-C2′) experiment. The parameters are identical to those listed above for the C1′-H1′ experiment with the exception of the changes described below. The direction of migration of the shaped ^{13}C and ^{15}N pulses during the second constant time period has been reversed. WURST2 decoupling on C2′ has been removed from the second constant-time period. An additional t_2 period has been added to the end of the second constant-time period with a composite 180 deg carbon pulse (striped) applied at full ^{13}C power in the middle of this incrementable delay. Selective WURST decoupling is applied during acquisition to effect ^{13}C decoupling of the C1′ nuclei without perturbing the C2′ nuclei. (B) C6-C5 (H6-C5) experiment. The parameters are identical to those listed above for the C6/8-H6/8 experiment with the exception of the changes described below. WURST2 decoupling on C5 has been removed from the second constant-time period. Selective WURST decoupling is applied during acquisition to effect ^{13}C decoupling of the C6/8 nuclei without perturbing the C5 nuclei.

provide good signal-to-noise and can be utilized to measure the desired couplings.

Materials and methods

Labeled DNA preparation

An 18 basepair DNA duplex with a core site for binding of the CBFα Runt domain (Berardi et al., 1999) has been labeled with ^{13}C and ^{15}N according to a modified version of a procedure described previously (Chen et al., 1998) using labeled dNTP's from Martek (Martek Biosciences Corporation, Columbia, MD). A description of the modifications made to the original methodology has been presented elsewhere (Yan and Bushweller, 2001).

Complex formation with CBFα(41–190)

The CBFα protein was prepared and the protein-DNA complex formed as described previously (Berardi et al., 1999).

NMR spectroscopy

All experiments were carried out on 500 and 600 MHz Varian Inova spectrometers equipped with Nalorac triple resonance gradient probes under conditions described previously for this complex (Berardi et al., 1999). All spectra were recorded on a sample of 0.4 mM protein-DNA complex with spectral widths of 11.1 ppm in ^{1}H, 6.7 ppm in ^{13}C and 49.6 ppm in ^{15}N on the 500 MHz spectrometer and of 10.8 ppm in ^{1}H, 6.6 ppm in ^{13}C and 49.3 ppm in ^{15}N on 600 MHz spectrometer, respectively. The pulse sequences and appropriate parameters are shown in Figures 1–3. All data was processed using the program PROSA (Guntert et al., 1992). Spectra were visualized using XEASY (Bartels et al., 1995). Peak positions were determined using the automated peak-picking routine supplied with XEASY. To quantitatively measure the C6/8-H6/8, C1′-H1′, H6/8-N, H1′-N, H6-C5 and H1′-C2′ couplings, the final spectra were processed to 8192 data points in the ^{1}H dimension (0.8 Hz/pt). For measurement of the C6/8-N, C1′-N, C6-C5 and C1′-C2′ couplings, the final spectra were processed to 1024 data points (1.0 Hz/pt) in the ^{13}C dimension after 3-fold linear prediction.

Measurement of $^{13}C1'$-$^{1}H1'$ and $^{13}C6/8$-$^{1}H6/8$ one-bond couplings

The 3D experiments in Figure 1 were recorded as $512(^{1}H)\times28(^{13}C)\times40(^{15}N)$ complex points ($t_{3\ max}$ = 79 ms, $t_{2\ max}$ = 28 ms and $t_{1\ max}$ = 13 ms) with 8 scans per increment and a 1.5 s recycle delay on the 600 MHz spectrometer. A total time of 17 h was used for each spectrum. The same experiments were recorded at 500 MHz with $512(^{1}H)\times22(^{13}C)\times50(^{15}N)$ complex points ($t_{3\ max}$ = 93 ms, $t_{2\ max}$ = 26 ms and $t_{1\ max}$ = 20 ms) with the same number of scans and recycle delay.

Measurement of $^{13}C1'$-$^{15}N1/9$ one-bond couplings and $^{1}H1'$-$^{15}N1/9$ two-bond couplings

The 3D experiment shown in Figure 2A was recorded with $512(^{1}H)\times24(^{13}C)\times42(^{15}N)$ complex points ($t_{3\ max}$ = 79 ms, $t_{2\ max}$ = 24 ms and $t_{1\ max}$ = 14 ms) with 24 scans per increment and a 1.5 sec recycle delay on the 600 MHz spectrometer. On the 500 MHz spectrometer, $512(^{1}H)\times22(^{13}C)\times44(^{15}N)$ complex points ($t_{3\ max}$ = 93 ms, $t_{2\ max}$ = 26 ms and $t_{1\ max}$ = 18 ms) were utilized with the same number of scans and recycle delay.

Measurement of $^{13}C6/8$'-$^{15}N1/9$ one-bond couplings and $^{1}H6/8$'-$^{15}N1/9$ two-bond couplings

The 3D experiment shown in Figure 2B was recorded as $512(^{1}H)\times26(^{13}C)\times40(^{15}N)$ complex points ($t_{3\ max}$ = 79 ms, $t_{2\ max}$ = 26.0 ms and $t_{1\ max}$ = 13 ms) with 24 scans per increment and a 1.5 s recycle delay on the 600 MHz spectrometer. On the 500 MHz spectrometer, $512(^{1}H)\times22(^{13}C)\times44(^{15}N)$ complex points ($t_{3\ max}$ = 93 ms, $t_{2\ max}$ = 26 ms and $t_{1\ max}$ = 18 ms) were utilized with the same number of scans and recycle delay. A total time of 48 h was used for each spectrum.

Measurement of one-bond $^{13}C1'$-$^{13}C2'$ and two-bond $^{1}H1'$-$^{13}C2'$ couplings

The 3D experiment shown in Figure 3A was recorded as $512(^{1}H)\times28(^{13}C)\times40(^{15}N)$ complex points ($t_{3\ max}$ = 79 ms, $t_{2\ max}$ = 28 ms and $t_{1\ max}$ = 13 ms) with 16 scans per increment and a 1.5 sec recycle delay on the 600 MHz spectrometer. On the 500 MHz spectrometer, $512(^{1}H)\times22(^{13}C)\times46(^{15}N)$ complex points ($t_{3\ max}$ = 93 ms, $t_{2\ max}$ = 26 ms, $t_{1\ max}$ = 18 ms) were utilized with the same number

of scans and recycle delay. A total time of ca. 30 h was used for each spectrum.

Measurement of one-bond $^{13}C6$-$^{13}C5$ and two-bond $^{1}H6$-$^{13}C5$ couplings

The 3D experiment shown in Figure 3B was recorded as $512(^{1}H)\times28(^{13}C)\times40(^{15}N)$ complex points ($t_{3\ max}$ = 79 ms, $t_{2\ max}$ = 28 ms and $t_{1\ max}$ = 13 ms) with 16 scans per increment and a 1.5 s recycle delay on the 600 MHz spectrometer. On the 500 MHz spectrometer, $512(^{1}H)\times22(^{13}C)\times46(^{15}N)$ complex points ($t_{3\ max}$ = 93 ms, $t_{2\ max}$ = 26 ms and $t_{1\ max}$ = 18 ms) were utilized with the same number of scans and recycle delay. A total time of ca. 30 h was used for each spectrum.

Results and discussion

Figures 1–3 show the MQ-HCN sequences utilized to measure the one bond C1′-H1′ and C6/8-H6/8 couplings (Figure 1), the one-bond C1′-N and C6/8-N couplings as well as the two-bond H1′-N and H6/8-N couplings (Figure 2), and the one-bond C1′-C2′ and C6-C5 as well as the two-bond H1′-C2′ and H6-C5 couplings (Figure 3). All the pulse sequences are generally based on the selective MQ-HCN experiments described previously by Sklenar and co-workers (Fiala et al., 1998). Since the MQ-HCN pulse sequence has been previously described in detail (Farmer et al., 1993, 1994; Sklenar et al., 1993a, b 1998; Tate et al., 1994; Marino et al., 1997; Fiala et al., 1998), only a brief description of each experiment is provided with a focus on the modifications employed to make possible measurement of the desired one- and two-bond couplings. The magnetization pathway for all the sequences can be described as:

$$^{1}\mathrm{HC} \xrightarrow{J_{\mathrm{C,H}}} {}^{13}\mathrm{C}^{1}\mathrm{H} - \mathrm{mq} \xrightarrow{J_{\mathrm{C,N}}} {}^{15}\mathrm{N}(t_1) \xrightarrow{J_{\mathrm{C,N}}}$$

$$^{13}\mathrm{C}^{1}\mathrm{H} - \mathrm{mq}(t_2) \xrightarrow{J_{\mathrm{C,H}}} {}^{1}\mathrm{HC}(t_3).$$

We have found the use of a ^{1}H spinlock during the constant-time periods rather than selective proton pulses to give very similar signal-to-noise so this has been incorporated into all the sequences in order to simplify the coding of the pulse sequences. We have also compared this version of the MQ-HCN experiment to TROSY versions of the HCN experiment (Fiala et al., 2000) and found it to provide a more uniform and therefore overall superior performance over all the base as well as ribose moieties in this large protein-DNA complexes we have been studying using 600 and 500 MHz spectrometers. In order to record the ^{13}C dimensions in these 3D experiments, it is necessary to remove the $^{13}C1'$-$^{13}C2'$ coupling in the H1′-C1′-N experiment and the $^{13}C6$-$^{13}C5$ coupling in the H6/8-C6/8-N experiment. This has been accomplished by means of selective WURST decoupling on the appropriate spectral regions. Figure 1 shows the sequences we have used for the measurement of $^{13}C1'$-$^{1}H1'$ and $^{13}C6/8$-$^{1}H6/8$ one-bond couplings ($J + D$). The only difference between the two experiments is the offset of the ^{13}C carrier and a small difference in the duration of the ^{13}C REBURP 180 degree pulses used during the constant-time periods. Removal of the ^{13}C decoupling during acquisition permits the detection of the doublet displaying the desired coupling in the acquisition dimension. Unlike protein amide NHs which show a clear difference in linewidth for the two lines of the doublet due to differential relaxation behavior, the proton lines of a $\{^{13}C\}$-^{1}H doublet do not display such a difference (Pervushin et al., 1998; Brutscher et al., 1998). This makes direct measurement in the acquisition dimension still favorable.

Perhaps more importantly, the 3D HCN provides the resolution necessary to accurately measure individual CH moieties. As pointed out in the Introduction, previous efforts utilizing 2D methods to measure a significant number of dipolar couplings in a 12 basepair labeled DNA oligonucleotide required the use of multiple alternatively labeled samples to obtain the necessary data (Tjandra et al., 2000). Our MQ-HCN based experiments take advantage of the dispersion afforded by the N nuclei to greatly improve the number of couplings that can accurately be measured. For the 18 basepair labeled DNA oligonucleotide utilized in these studies, all of the C1′-H1′ resonances are found in a small window of 0.8 ppm in ^{1}H and 3.9 ppm in ^{13}C. Using the methods described herein, 95% of the C1′-H1′ resonances identified in a ^{13}C-^{1}H HSQC could have their associated couplings measured at 600 MHz. Measurement of these couplings by 2D methods, such as α,β-TROSY (Brutscher et al., 1998), would be difficult due to the poor dispersion and would only become worse with increasing size of the oligonucleotide or decreasing field strength. Similarly for the C6/8-H6/8 moieties, the resolution afforded by the 3D makes possible the measurement of these couplings where 2D experiments would be more difficult. In addition, the favorable dispersion associated with

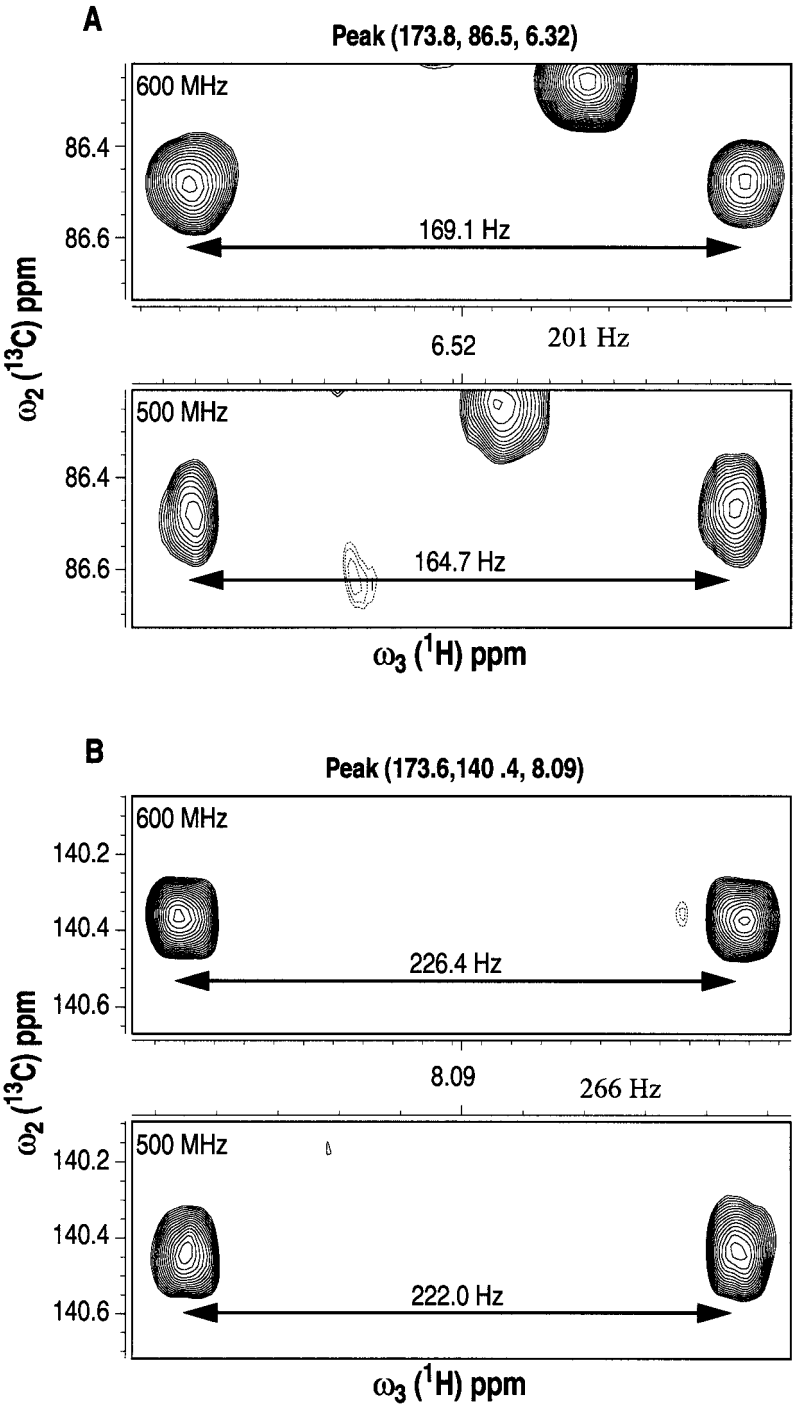

Figure 4. Selected strips from each of the experiments shown in Figure 1 displaying the measured couplings at 500 and 600 MHz. (A) Selected strips from the C1′-H1′ experiments recorded at 500 and 600 MHz. A width of 200 Hz in the ^{1}H dimension has been used for each strip. (B) Selected strips from the C6/8-H6/8 experiments recorded at 500 and 600 MHz. A width of 250 Hz in the ^{1}H dimension has been used for each strip. The $(J + D)$ couplings were measured and the values are indicated.

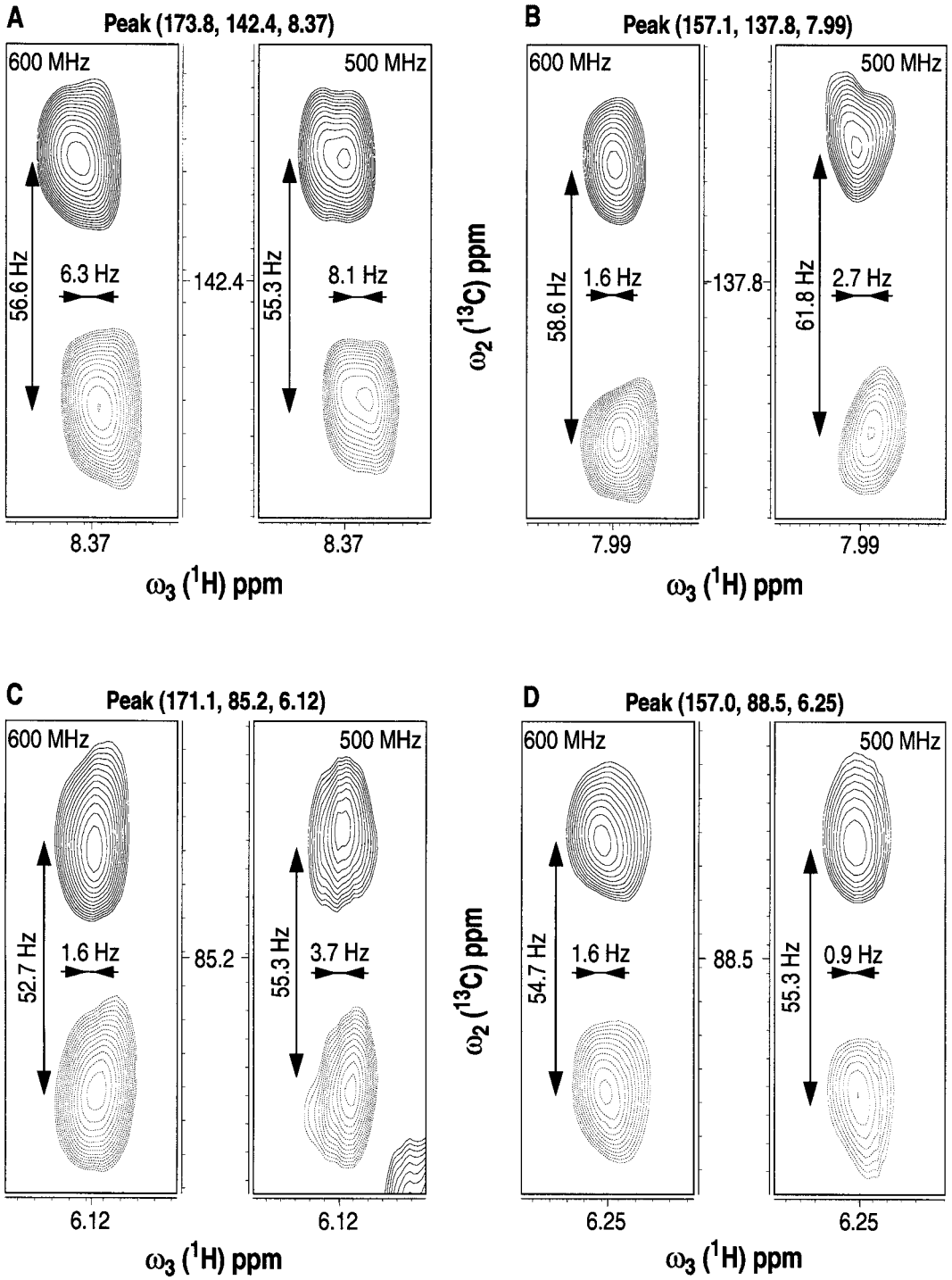

Figure 5. Selected strips from each of the experiments shown in Figure 2 displaying the measured couplings at 500 and 600 MHz. (A), (B) Selected strips from the C6/8-N (H6/8-N) experiments recorded at 500 and 600 MHz. (C), (D) Selected strips from the C1′-N (H1′-N) experiments recorded at 500 and 600 MHz. All strips are shown with 60 Hz (^{1}H) × 105 Hz (^{13}C) windows. The measured one-bond C1′-N and C6/8-N couplings ($(\kappa + 1) \times (J + D)$) and two-bond H1′-N and H6/8-N couplings ($J + D$) are indicated.

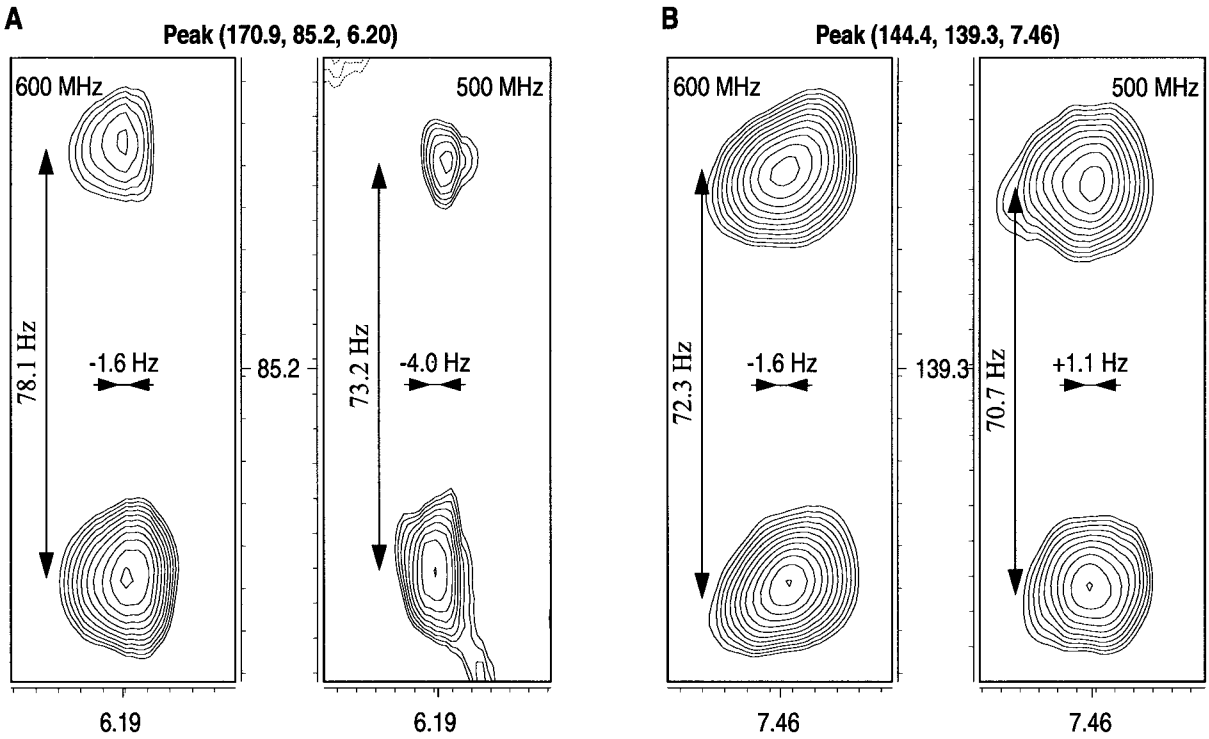

Figure 6. Selected strips from each of the experiments shown in Figure 3 displaying the measured couplings at 500 and 600 MHz. (A) Selected strips from the C1′-C2′ (H1′-C2′) experiments recorded at 500 and 600 MHz. (B) Selected strips from the C6-C5 (H6-C5) experiments recorded at 500 and 600 MHz. All strips are shown with 60 Hz (^{1}H) × 112 Hz (^{13}C) windows. The measured one-bond couplings C1′-C2′ ($2*(J+D)$) and C6-C5 ($J+D$) and two-bond H1′-C2′ and H6-C5 couplings ($J+D$) are indicated.

these 3D methods make it possible to utilize lower field strength data for this size oligonucleotide and to extend the size of the oligonucleotides for which meaningful dipolar coupling data can be obtained.

Figure 4 shows strips for selected C1-H1′ and C6/8-H6/8 moieties obtained at 500 and 600 MHz using these sequences. Previous experiments had found that the ternary complex of the DNA, CBFβ, and the CBFα Runt domain displays alignment on its own, so we are currently comparing values obtained at several field strengths to assess the magnitude of this magnetic anisotropy. The differences between data obtained at 600 and 500 MHz are illustrated in Figure 4.

Figure 2 shows the E. COSY-based MQ-HCN sequences used for the measurement of C1′-N and C6/8-N one-bond couplings. This sequence resembles the TROSY-based HNCO developed by Kay and coworkers (Yang et al., 1999) for the measurement of protein backbone N-CO couplings. Similar to that sequence, two crosspeaks with a separation of $|(1+\kappa)^1 J_{CN}|$ and opposite in phase, are obtained in the ^{13}C dimension for each C1′ or C6/8 resonance. Due to the relatively small $^1J_{CN}$ coupling (ca. 10–12 Hz), we have chosen to employ a value of κ of 4, resulting in a 5-fold amplification of the $^1J_{CN}$ coupling. This has proven to be a reasonable compromise between the need for an adequate magnitude to accurately measure the peaks and the losses due to T_2 relaxation over the course of these relatively long delay periods. Figure 5 shows selected strips from the C1′-N and C6/8-N experiments recorded at 500 and 600 MHz. In addition to the one-bond C1′-N and C6/8-N couplings, these experiments also provide a measure of the two-bond H1′-N and H6/8-N couplings, as illustrated in Figure 5. The relaxation behavior of the CH moieties in the MQ-HCN with a spinlock on ^{1}H has proven to be excellent resulting in very good signal-to-noise despite the substantial length of the delays in these sequences, much like the use of TROSY-based methods in the sequence developed by Kay and co-workers provides the needed performance for large protein systems. There are only minor differences between the sequences used for measurement of C1′-N and C6/8-N couplings, with the exception of the selective 180 deg pulse applied to the N7 of A and G to eliminate evolution of the C8-N7 coupling during this time. For this purpose, we have

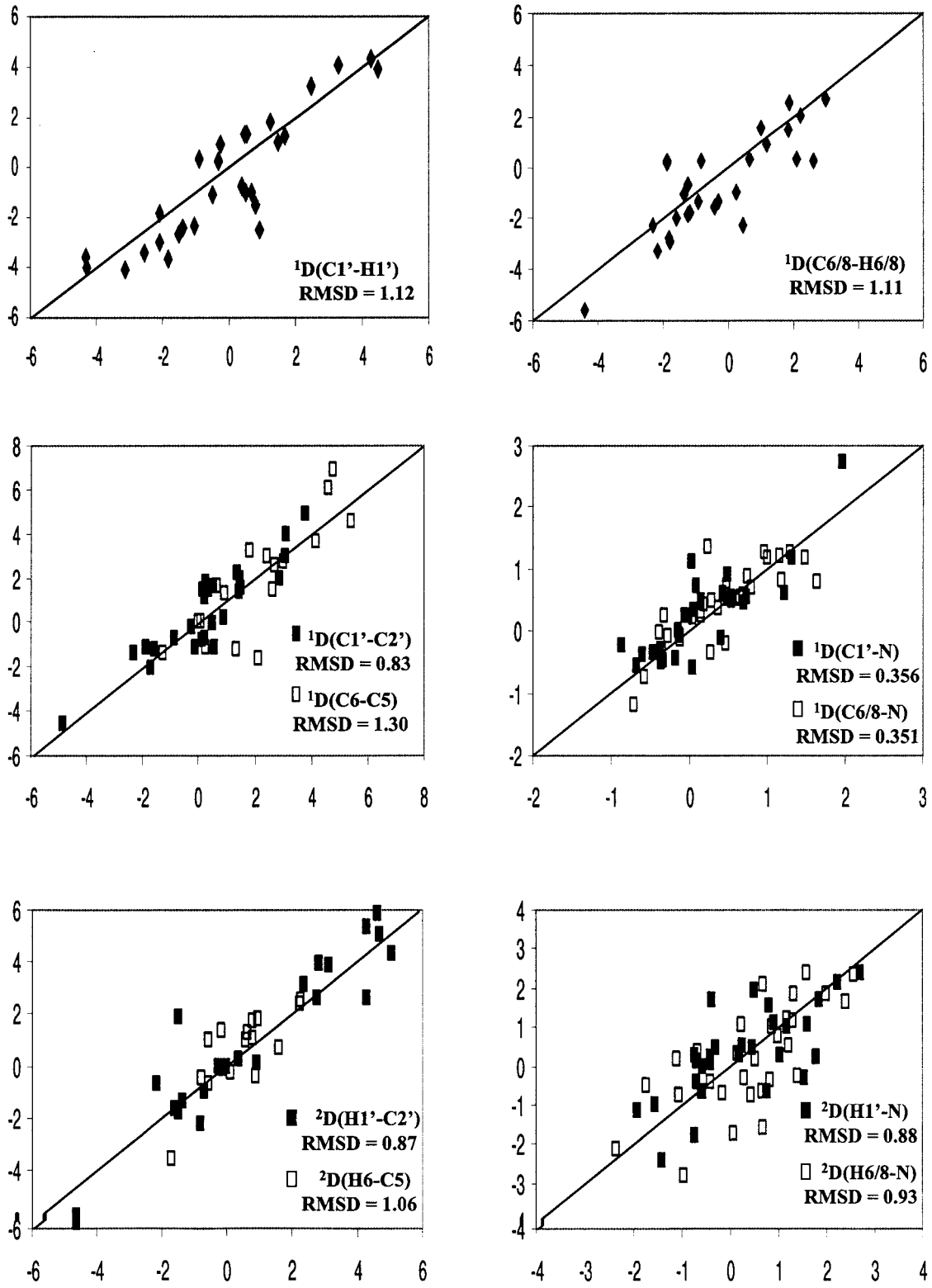

Figure 7. Correlations between D_{ij} (Hz) values measured from repeat experiments. Values were calculated as $D_{ij}(600) - D_{ij}(500)$. The pair-wise RMSD values obtained are indicated in the lower right-hand corner of each plot.

employed an ISNOB3 (Kupce et al., 1995) pulse in order to limit the pulse duration and reduce the number of points that need to be back-predicted in the ^{13}C dimension.

Figure 3 shows the pulse sequences used for the measurement of the one-bond ^{13}C1′-^{13}C2′ and ^{13}C6-^{13}C5 couplings as well as the two-bond ^{1}H1′-^{13}C2′ and ^{1}H6-^{13}C5 couplings. Removal of the C2′ or C5 decoupling from the pulse sequences shown in Figure 1 results in the splitting of the C1′ and C6 resonances in the ^{13}C dimension due to the one-bond ^{13}C1′-^{13}C2′ and ^{13}C6-^{13}C5 couplings, respectively. In the case of the ^{13}C6-^{13}C5 coupling, the large magnitude of this coupling (ca. 67 Hz) permits direct measurement without amplification of the coupling, much as ^{13}CO-^{13}Cα couplings have been measured in proteins using TROSY-HNCO pulse sequences (Yang et al., 1999). In the case of the ^{13}C1′-^{13}C2′ coupling, the smaller magnitude (ca. 43 Hz) makes it more difficult to obtain the separation necessary for accurate measurements. For this reason, we have employed accordion spectroscopy to double the observed separation between the two peaks, as shown in Figure 3. Again, due to the very good relaxation behavior of the MQ state for the CH moieties, we can obtain very good signal-to-noise in these experiments as well. Figure 6 shows selected strips from the C1-C2′ and C6-C5 MQ-HCN experiments, illustrating the excellent performance. In addition to the ^{13}C1′-^{13}C2′ and ^{13}C6-^{13}C5 couplings, these experiments also provide a measure of the ^{1}H1′-^{13}C2′ and ^{1}H6-^{13}C5 two-bond couplings, as illustrated in Figure 6. In order to obtain these couplings, the ^{13}C decoupling during acquisition has been tailored to only decouple the C1′ and C6 regions of the ^{13}C spectrum without perturbing the C2′ and C5 regions, respectively.

In order to characterize the attainable accuracy of the various couplings we have measured, the data has been collected on the 500 and 600 MHz spectrometers on 2 separate occasions, several months apart. Figure 7 shows plots of the measured differences between the 2 field strengths obtained from the 2 different measurements, which permits a measurement of the RMSD for each. Peaks that were resolved in the spectra at 500 and 600 MHz have been utilized for the RMSD determinations. Based on a typical range of ca. 40 Hz for protein amide NH dipolar couplings (see for example Bayer et al., 1999) in the presence of some medium causing weak alignment, we would obtain a range of ca. 80 Hz for the C1′-H1′ and C6/8-H6/8 couplings assuming an isotropic distribution. The ranges of the various other couplings measured by our pulse sequences would then be: C1′-N and C6/8-N19 (ca. 3 Hz), H1′-N19 and H6/8-N19 (ca. 3 Hz), C1′-C2′ (ca. 7 Hz), C6-C5 (ca. 10 Hz), H1′-C2′ and H6-C5 (ca. 8 Hz). The RMSD values indicated in Figure 7 indicate that all of the measured couplings will give statistically meaningful dipolar coupling information under these type of conditions.

Conclusions

In summary, we have developed a suite of MQ-HCN based experiments for the measurement of a total of 10 one- and two-bond couplings centered on the C1′ and C6/8 nuclei in labeled nucleic acids. The resolution afforded by the more well-dispersed N nuclei in these experiments makes possible a large number of measurements which would be difficult to obtain by other methods. The highly favorable relaxation properties of the CH multiple quantum state used in these experiments results in excellent signal-to-noise, even for very large complexes. We have demonstrated the applicability of these sequences by making measurements on a labeled 18 bp DNA duplex in a 47 kDa ternary complex consisting of the DNA, CBFβ, and the CBFα Runt domain.

Acknowledgements

J.H.B. is supported by grants from the United States Public Health Service from the Institute for Allergy and Infectious Disease. We wish to thank Jeff Peng for a number of useful discussions.

References

Bartels, C., Xia, T., Billeter, M., Guntert, P. and Wuthrich, K. (1995) *J. Biomol. NMR*, **6**, 1–10.

Bayer, P., Varani, L. and Varani, G. (1999) *J. Biomol. NMR*, **14**, 149–155.

Berardi, M., Sun, C., Zehr, M., Abildgaard, F., Peng, J., Speck, N.A. and Bushweller , J.H. (1999) *Structure*, **7**, 1247–1256.

Brutscher, B., Boisbouvier, J., Pardi, A., Marion, D. and Simorre, J. (1998) *J. Am. Chem. Soc.*, **120**, 11845–11851.

Chen, X., Mariappan, S.V.S., Kelley, J.J., Bushweller, J.H., Bradbury, E.M. and Gupta, G. (1998) *FEBS Lett.*, **436**, 372–376.

Farmer, B.T., Muller, L., Nikonowicz, E.P. and Pardi, A. (1993) *J. Am. Chem. Soc.*, **115**, 11040–11041.

Farmer, B.T., Muller, L., Nikonowicz, E.P. and Pardi, A. (1994) *J. Biomol. NMR*, **4**, 129–133.

Fiala, R., Czernek, J. and Sklenar, V. (2000) *J. Biomol. NMR*, **6**, 291–302.

Fiala, R., Jiang, F. and Sklenar, V. (1998) *J. Biomol. NMR*, **12**, 373–383.

Guntert, P., Dotsch, V., Wider, G. and Wuthrich, K. (1992) *J. Biomol. NMR*, **2**, 619–629.

Kupce, E., Boyd, J. and Campbell, I.D. (1995) *J. Magn. Reson.*, **106B**, 300.

Marino, J.P., Diener, J.L., Moore, P.B. and Griesinger, C. (1997) *J. Am. Chem. Soc.*, **119**, 7361–7366.

Pervushin, K., Riek, R., Wider, G. and Wuthrich, K. (1998) *J. Am. Chem. Soc.*, **120**, 6394–6400.

Sklenar, V., Dieckmann, T., Butcher, S.E. and Feigon, J. (1998) *J. Magn. Reson.*, **130**, 119–122.

Sklenar, V., Peterson, R.D., Rejante, M.R., Wang, E. and Feigon, J. (1993a) *J. Am. Chem. Soc.*, **115**, 12181–12182.

Sklenar, V., Peterson, R.D., Rejante, M.R. and Feigon, J. (1993b) *J. Biomol. NMR*, **3**, 721–727.

Smallcombe, S.H., Patt, S.H. and Keifer, P.A. (1995) *J. Magn. Reson.*, **A117**, 295–303.

Tate, S., Ono, A. and Kainosho, M. (1994) *J. Am. Chem. Soc.*, **116**, 5977–5978.

Tjandra, N. and Bax, A. (1997) *J. Am. Chem. Soc.*, **119**, 8076–8082.

Tjandra, N., Tate, S.-I., Ono, A., Kainosho, M. and Bax, A. (2000) *Science*, **278**, 1111–1114.

Yan, J. and Bushweller, J.H. (2001) *Biochem. Biophys. Res. Commun.*, **284**, 295–300.

Yang, D., Venters, R. A., Mueller, G. A., Choy, W.Y. and Kay, L.E. (1999) *J. Biomol. NMR*, **14**, 333–343.